Science of the Total Environment 880 (2023) 163035

Contents lists available at ScienceDirect

Science of the Total Environment

journal homepage: www.elsevier.com/locate/scitotenv

Limited access to oxygen reduces the release of harmful trace elements from submerged alum shale debris

Frøydis Meen Wærsted [a,b,*], Estela Reinoso-Maset [a], Brit Salbu [a], Lindis Skipperud [a]

[a] Centre for Environmental Radioactivity (CERAD CoE), Faculty of Environmental Sciences and Natural Resource Management, Norwegian University of Life Sciences, Elizabeth Stephansens vei 29, 1433 Aas, Norway
[b] Norwegian Geotechnical Institute, P. O. Box 3930, Ullevål Stadion, 0806 Oslo, Norway

HIGHLIGHTS

- Alum shale can produce acid rock drainage when exposed to air and water.
- Leaching from alum shale was investigated under atmospheric and low O_2 conditions.
- Results are compared to measurements from disposal site.
- Pyrite oxidation and element leaching rates were slower under low O_2 conditions.
- The results support waste rock storage in stagnant water to avoid acid rock drainage.

GRAPHICAL ABSTRACT

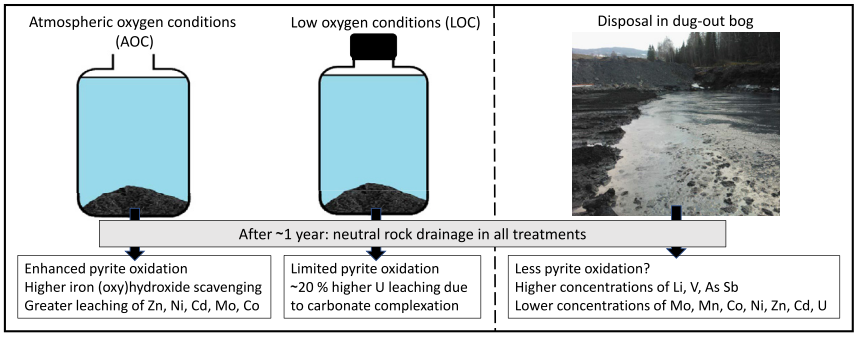

ARTICLE INFO

Editor: Filip M.G.Tack

Keywords:
Alum/black shale
Oxygen levels
Pyrite oxidation
Acid/neutral rock drainage
Naturally occurring radioactive materials (NORM)
Trace elements

ABSTRACT

Construction and mining activities in acid-producing alum shale regions often produce large volumes of crushed rock. Disposal under groundwater level (e.g., a bog) may minimize oxygen access. In this study, the effect of varying oxygen access on the leaching potential of alum shale was investigated by submerging tunnel construction rock debris in synthetic rainwater under atmospheric (AOC) and low oxygen conditions (LOC) for 52 weeks. The sulphate increase and nitrate decrease in the leachates suggested that pyrite (FeS_2) in the alum shale was oxidized, but carbonates originating from calcite dissolution provided sufficient buffering capacity (leachate pH ~7.7 over 52 weeks), resulting in neutral rock drainage. Less available oxygen led to significantly lower production of sulphate and acid from pyrite oxidation, reducing the release of harmful elements. Under LOC, the leaching of Mo, Co, Ni, Zn and Cd was 2–4 times lower than under AOC and the lower buffering requirement diminished the release of Ca as well as divalent cations (Mg, Sr, Mn) likely present as impurities in calcite. Contrastingly, limited pyrite oxidation led to less oversaturation with respect to $BaSO_4$ and lower release of Fe in the LOC leachates. Thus, co-precipitation of ^{226}Ra was inhibited and scavenging of leached V, As and Sb by newly formed $Fe(OH)_3$ was not as dominant as in the AOC systems. Leaching of U was ~20 % higher under LOC likely due to enhanced complexation by dissolved carbonate. In general, element leaching rates were slower under low O_2 levels. Characterization of water collected at the disposal site after ~1.2 years of discarding tunnel materials showed that the weathering of debris submerged in the open, water-filled pond occurred similarly to leaching under low oxygen conditions. Overall, these results highlight the importance of minimal oxygen access or anaerobic conditions when acid-producing rock waste is stored under water.

* Corresponding author at: Norwegian Geotechnical Institute, P. O. Box 3930, Ullevål Stadion, 0806 Oslo, Norway.
E-mail addresses: froydis.wersted@ngi.no (F.M. Wærsted), estela.reinoso.maset@nmbu.no (E. Reinoso-Maset), brit.salbu@nmbu.no (B. Salbu), lindis.skipperud@nmbu.no (L. Skipperud).

http://dx.doi.org/10.1016/j.scitotenv.2023.163035
Received 3 January 2023; Received in revised form 16 March 2023; Accepted 20 March 2023
Available online 24 March 2023
0048-9697/© 2023 The Authors. Published by Elsevier B.V. This is an open access article under the CC BY license (http://creativecommons.org/licenses/by/4.0/).

1. Introduction

Crushed rock produced in mining and construction areas is a potential source for naturally occurring radioactive materials (NORM) and other potentially harmful trace elements being released into the surrounding environment. Processing and storage of rock in the environment can alter its physical properties as well as the chemistry of elements contained in the rock, which can lead to increased mobility, ecosystem transfer and, ultimately, biological uptake and negative effects to biota. Thus, proper storage of acid-producing rock waste is needed, but often difficult and expensive to achieve. Local storage may be preferred as it can eliminate large transportation costs and reduce weathering of debris during transit. For example, at Gran in Hadeland, Norway, alum shale and other rocks from tunnel construction were reused locally to fill an excavated bog, where the debris was submerged in water and the disposal site was covered with a multilayer surface coating (crushed rock, silt/peat, asphalt) varying with the final use of the area, to reduce access to air (see Fjermestad et al. (2018) for details). However, if the disposal site has not been properly sealed, oxygenated water could enter and thereby oxidise the debris, resulting in contaminated water leaching into the downstream river Vigga and potentially detrimental effects on the local environment.

Alum shale is a Cambro-Ordovician black mudrock (sedimentary rock) formed under reducing conditions, containing silicate minerals, organic matter (kerogen), as well as sulphide and carbonate phases (Falk et al., 2006; Owen et al., 1990; Pabst et al., 2017). Alum shale is enriched in elements of environmental concern, including Cd, Co, Cu, As, Ni, Zn, V, Mo, Ba and U, and due to secular equilibrium between ^{238}U and its daughter nuclides (IAEA, 2014), the highly radiotoxic radionuclide ^{226}Ra will also be present in unweathered alum shale. Alum shales are typically acid-generating rocks, i.e., their neutralization potential (NP) to acidification potential (AP) ratio is lower than 1 (Pabst et al., 2017). The NP is mainly provided by carbonate phases, while the AP is normally originating from sulphide-containing minerals such as pyrite (FeS_2) and pyrrhotite ($Fe_{1-x}S$, x = 0–0.2). Thus, when alum shale is exposed to air and water, oxidation of sulphide minerals will produce acid, resulting in acid rock drainage containing high levels of NORM and stable, potentially harmful elements.

Changes in the rock system conditions, e.g., exchange of porewater or a decrease in pH, may further enhance alum shale weathering and the consequent release of elements of environmental concern. For example, 1–2 orders of magnitude higher concentrations of Cd, Cu, Ni and Zn and of Cu and Fe were released from alum shale following a pH drop in the leachates below 5 (Falk et al., 2006) and below 3 (Jeng, 1992), respectively. At such low pH, the solubility of Al, Th, and U is favoured and the release of a series of elements is expected to increase (Hindar and Nordstrom, 2015; Landa, 2007), whereas scavenging by Fe (oxy)hydroxides will be minimal (Jeng, 1992; Singer and Stumm, 1970). Furthermore, the presence of organic matter can play an important role in changing the speciation, and thus mobility, of elements with high affinity for humic substances, such as Ni, Zn, Cu, Cd, Pb and U (Moulin et al., 2004). Therefore, the weathering of and leaching from alum shale will depend on the storage conditions. The release of harmful elements is expected to occur to a higher extent under atmospheric oxygen conditions compared to conditions when limited oxygen is available. Presence of carbonates can buffer acid production from pyrite oxidation, but the pH will drop if the available carbonates are consumed. Nevertheless, even without a drop in pH, radionuclides and metals incorporated in alum shale can be released during oxidation, leading to neutral rock drainage (NRD) (Vriens et al., 2019).

The present work focused on the release of trace elements and NORM of relevance to humans and the environment from alum shale debris collected during construction works at Gran, Norway, by assessing its stability under different simulated storage conditions. Freshly crushed alum shale was leached with synthetic rainwater under atmospheric oxygen conditions (AOC) and low oxygen conditions (LOC) for 52 weeks. The leaching behaviour of 41 elements was investigated and results from the two treatments were compared to water collected at the disposal site at Gran and to environmental quality standards.

2. Materials and methods

2.1. General

Type I water (ASTM D1193-91 standard specifications) and analytical grade chemicals were used unless otherwise noted.

2.2. Site description and sampling

At Gran, Hadeland, Norway (Fig. 1), tunnel blasts with >10 % alum shale were reused as filling material under the road to be constructed at the southern entrance of the tunnel (Fjermestad et al., 2018). To ensure continuous submerging of the blast materials, the disposal site was an excavated bog below groundwater level with a slow exchange of water draining into the small river Vigga. In total, about 66,500 m^3 of alum shale and 10,500 m^3 of other black shales were placed in the bog.

Alum shale debris from tunnel construction was collected on 19/05/2015 from a blast in the alum shale formation executed on the same day. Handheld XRF (Niton™ XL3t GOLDD+, Thermo Scientific) was used to ensure that uranium-rich material was collected. The material was stored for 6 months prior to experiments. For comparison with laboratory experiments, water from the disposal site pond was also sampled (Fig. 1). At the time of sampling, i.e., 1 year and 2 months into the tunnel construction, disposal and storage of masses was still ongoing and the site was an open pond. Conductivity and pH were measured directly in the pond water with a handheld multi-meter (Multi series, WTW). Unfiltered samples were taken for analysis of anions and total organic carbon (TOC), while for elemental analysis by inductively coupled plasma mass spectrometry (ICP-MS), the pond water was filtered in situ with 0.45 μm membrane filters (Millipore) and acidified to 5 % (*v/v*) with ultrapure HNO_3. All water samples were stored in the dark at 4 °C until analysis.

2.3. Leaching experiments

Alum shale pieces >2 cm were crushed with a jaw crusher to get fresh rock surface, sieved through a 2 mm mesh and stored in under N_2 atmosphere for <72 h until the start of the experiment. Crushing was done in air to simulate tunnel construction operations.

Batch experiments were performed with 150 g crushed rock debris and 1.5 L synthetic rainwater with the same average composition (pH 4.9 and low content of ions; Table S1) as precipitation monitored during 2010–2014 in Hurdal, 27 km west of the sampling site (Fig. 1) (Aas et al., 2015). Three samples were prepared in 2 L Nalgene polypropylene bottles (Thermo Scientific) and kept open to the atmosphere (atmospheric oxygen conditions; AOC). Another three samples were prepared with N_2 flushed rainwater (~1.5 h, 0.01 mg L^{-1} O_2) in heavy-duty vacuum bottles with installed septum lids (2 L, Nalgene polypropylene; Thermo Scientific) and kept under N_2 atmosphere (low oxygen conditions; LOC) inside bags of oxygen-excluding material (FireDebris Tubular Rollstock, Ampac). This set-up did not completely exclude oxygen; thus, oxygen in both water and gas phase was measured at each sampling point. To monitor contamination and other unintended experimental effects, one blank sample per treatment consisting of only synthetic rainwater (no debris) was prepared in parallel and treated, sampled, and analysed in the same manner.

The batch samples were kept in the dark at 10 °C for 52 weeks and shaken by hand 2–3 times per week to suspend all debris in the rainwater. For leachate analyses (Section 2.5), water aliquots were sampled at 1 h, 24 h, and 1, 4, 12, 28 and 52 weeks after batch preparation. The extracted volume was replaced with fresh synthetic rainwater, which resulted in a total of 20 % of the volume being exchanged by the end of the experiment. For the LOC systems, sampling of water and gas was carried out inside the N_2-filled glove bag. The gas phase was sampled through the septum lids using a syringe before each water sampling and at additional time points, but since the gas phase was exchanged during the water sampling, the measured O_2, N_2, CH_4 and CO_2 levels (Agilent 7890A Network Gas Chromatograph) could not be considered as undisturbed, continuous development

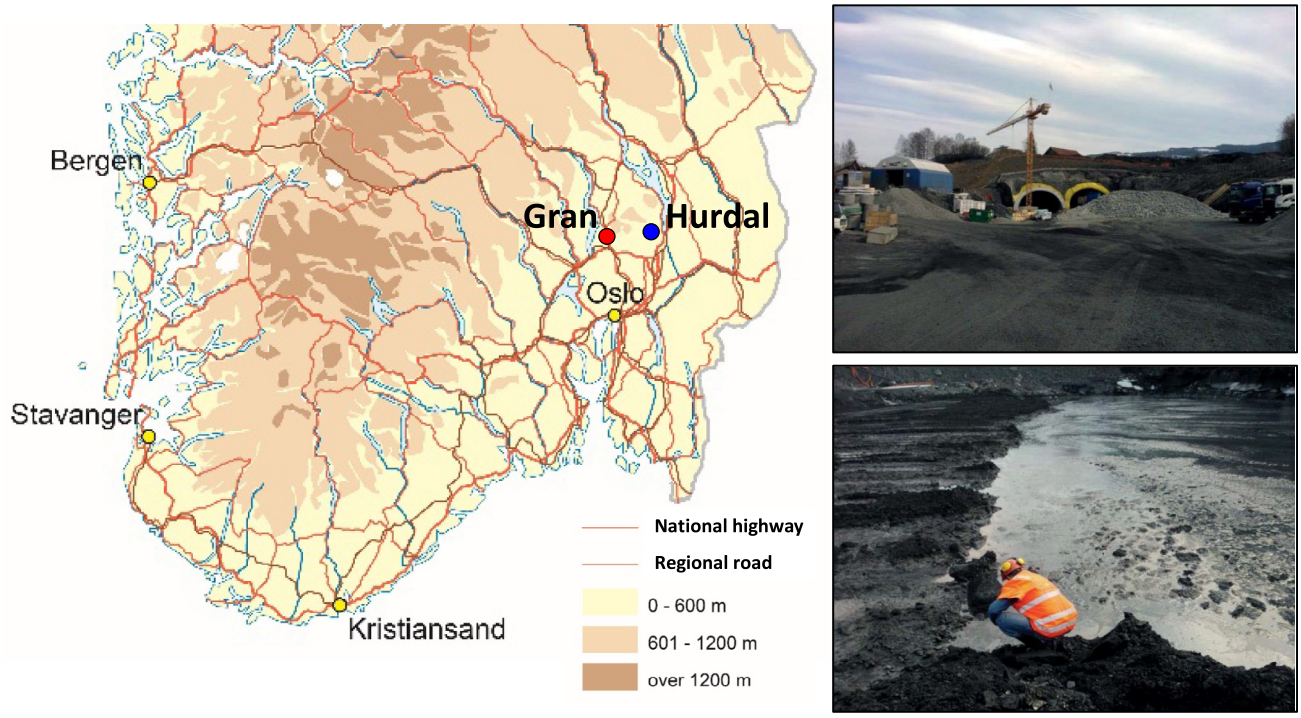

Fig. 1. Location of Gran, where alum shale from the tunnel construction material (*top right*) and water from the disposal site (*bottom right*) were collected, and Hurdal, the reference site for the rainwater composition used in the alum shale leaching experiments. Ground map obtained from Kartverket (www.kartverket.no) and used under Creative Commons Attribution ShareAlike 3.0.

over time. Subsamples of the alum shale debris before and after leaching were also collected for solid phase characterization (Section 2.4).

2.4. Alum shale characterization

Organic matter (OM) in the debris was estimated from loss-on-ignition (LOI; 550 °C, overnight), whereas total organic/inorganic carbon (TOC/TIC) was measured by coulometry. TOC content was measured only in the starting material. Particle size distribution was determined in organic-free debris (H_2O_2 heated; 10 g) by wet sieving through a 63 μm mesh to exclude the sand fraction. Silt (63–2 μm) and clay (< 2 μm) fractions were separated by sedimentation according to Stokes' law. Air dried debris was analysed by powder X-ray diffraction (XRD) on a D8 Discover (Bruker), and diffractograms were fitted for qualitative mineral composition assessment and Rietveld quantitative phases analysis using TOPAS software and a reference spectra library.

Total element concentrations in the debris (0.25 g) were determined in triplicate by ICP-MS after microwave-assisted acid digestion (260 °C, 40 min, Milestone UltraCLAVE; Rh as internal standard). The following acid mixtures were applied: i) 5 mL HNO_3 (for Li, P, S, Ca and Fe), ii) 5 mL HNO_3 + 1 mL HF (for Mn, Cu, Zn, As, Mo, Cd, Sn, Sb and U), and iii) 2 mL HNO_3 + 4 mL H_3PO_4 (for Be, Na, Mg, Al, K, V, Cr, Co, Ni, Sr, Ba, La, Ce, Pr, Nd, Sm, Eu, Gd, Dy, Ho, Er, Tm, Yb, Lu, Pb, Ra and Th). Certified reference materials NIST 2709a San Joaquin soil and NSC ZC 73007 soil (with the 3 acid mixtures), NIST 2710a Montana I soil (only with HNO_3), NSC DC 73325 soil (only with HNO_3 + HF), and IAEA-314 sediment and IAEA-448 soil (only with HNO_3 + H_3PO_4) were digested and measured in parallel. Results for all reference materials where within the uncertainties of certified values.

2.5. Aqueous phase analyses

Collected leachate aliquots were divided into different subsamples. Oxygen concentrations (FDO® 925 Optical Dissolved Oxygen Sensor), conductivity, oxidation-reduction potential (ORP) and pH were measured immediately after sampling on untreated subsamples using a handheld multi-meter (Multi series, WTW). E_h was calculated from ORP according to instructions from producer. Subsamples for alkalinity, dissolved organic carbon (DOC), anion and elemental analyses were immediately filtered using 0.45 μm polyethersulfone membrane syringe units (VWR). In addition, subsamples from 1 h, 4, 12, 28 and 52 weeks were filtered through 10 kDa Amicon® Ultra-15 centrifugal filters (Merck Millipore) for low molecular mass (LMM) components analysis. Samples for ICP-MS analysis (i.e., 0.45 μm and LMM subsamples) were acidified with ultrapure HNO_3 to 5 % *v/v*. All samples were stored in the dark at 4 °C until analysis.

Alkalinity was measured by colorimetric titration to pH 4.5 (ISO 9963-1:1994). Anions were quantified by ion chromatography (Lachat IC5000 system, Dionex™ IonPac™ AS22-Fast IC column, Dionex AMMS™ 300 ion suppressor, Thermo Scientific). TOC/DOC was determined with a TOC-VCPN analyser (Shimadzu).

Acidified subsamples of synthetic rainwater, alum shale leachates, and digested alum shale debris were analysed with respect to Li, Be, Na, Mg, Al, P, S, K, Ca, V, Cr, Mn, Fe, Co, Ni, Cu, Zn, As, Sr, Mo, Cd, Sn, Sb, Ba, La, Ce, Pr, Nd, Sm, Eu, Gd, Dy, Ho, Er, Tm, Yb, Lu, Pb, Th and U using an Agilent 8800 triple quadrupole ICP-MS with He, O_2 or no gas in the collision/reaction chamber. Rhodium (for all except digested samples) and Ge, In, Ir and Bi (for all) were added online as internal standards, and an in-house standard covering all analysed elements except Sn was used to check the measurement accuracy on each analysis day. The disposal site water was analysed with respect to Li, Be, Na, Mg, Al, S, K, Ca, V, Cr, Mn, Fe, Co, Ni, Cu, Zn, As, Sr, Mo, Cd, Sn, Sb, La, Pb, Th and U following the same ICP-MS methodology. ^{226}Ra was measured in leachates and digested alum shale with an Agilent 8900 triple quadrupole ICP-MS using N_2O as reaction gas as described in Wærsted et al. (2018).

2.6. Data treatment

The acidification and neutralization potentials (AP and NP) of the alum shale debris were estimated by assuming that all S in the rock comes from sulphides behaving like pyrite and that the measured carbonates behave

like calcite, with each mole of calcite neutralizing two moles of protons (Lawrence and Wang, 1996). Geochemical characterization of the alum shale was performed by comparing measured elemental concentrations, TIC/TOC levels, Fe to S ratios, and estimated AP and NP with an existing database of Cambro-Ordovician black mudrocks from the Oslo region, Norway (Pabst et al., 2017). For further explanation and plots see Section 1.2 in the SI.

To compare with measured alkalinity, the solubility of calcite (K_{sp} = $5{\cdot}10^{-9}$) and measured (LOC samples) or atmospheric (AOC samples) CO_2 concentrations were applied in solubility calculations (as explained in vanLoon and Duffy (2011) to estimate the alkalinity at the experimental conditions. Contamination of Zn, V and Ba was observed in experimental blank samples; therefore, average concentrations of these elements were subtracted from leachate concentrations of the corresponding treatments. Moreover, at 28 weeks, one of the LOC replicate samples showed an unexpectedly high level of O_2 in the aqueous and gas phases, and the leached concentrations of several elements were similar to the AOC samples. This replicate was hence excluded from the 28- and 52-week LOC data averages. The percentage of leached mass for each element after 52 weeks was calculated as $\frac{mass\ in\ solution}{mass\ in\ starting\ material} \times 100$ and significant differences between treatments were evaluated by *t*-tests in Excel.

3. Results

3.1. Alum shale characterization

The alum shale debris was mostly in the sand-size range, with smaller fractions of silt- and clay-sized particles (Table 1). X-ray diffractograms of the alum shale were best fitted with muscovite ($KAl_2(AlSi_3O_{10})(F,OH)_2$) and quartz ($SiO_2$) as the main mineral phases and a smaller contribution of pyrite (FeS_2) and calcite ($CaCO_3$) (Table 1; see Section 1.3 in the SI for all quantification results and diffractograms). The pyrite fraction was somewhat lower than the 4–13 % previously reported for three Norwegian alum shales (Jeng, 1991). Amorphous material was also detected, and about half was accounted for by the OM. The debris had 8.9 % TOC and 0.29 % TIC (Table 1), the latter being similar to other acid-producing black shales in Norway (Pabst et al., 2017).

The most abundant elements in the alum shale were K, Mg, Ca, Fe, Al, and S (9–79 g kg^{-1}, Table 2). Potassium and Al were accounted for by the muscovite, while 75 % of the Ca and all TIC corresponded to the calcite fraction in the debris. Note that the high variability in Ca concentration (36 % RSD; Table 2) suggested heterogenous distribution of calcite, likely due to the presence of carbonate nodules in the rock (Wærsted, 2019). The pyrite fraction accounted for 51 % of the total Fe in the debris and 60 % of the total S; the remaining S could be present as sulphates or sulphides associated with Fe or other cations, or as part of the organic matter. Sodium, Sr, Ba, V, Cr, Mo, Mn, Ni, Cu, Zn, P and U were present at lower concentrations (0.1–3 g kg^{-1}), while Li, Be, Co, Cd, Sn, Pb, As, Sb, rare earth elements and Th concentrations varied from 0.7 to 92 mg kg^{-1}, and the ^{226}Ra concentration was 35 ng kg^{-1}. The present elemental composition falls within the rather wide concentration range at other Scandinavian locations (Falk et al., 2006; Jeng, 1991; Jeng, 1992; Lavergren et al., 2009; Pabst et al., 2017). The corresponding activity concentrations of ^{232}Th, ^{238}U, and ^{226}Ra were 0.60, 1.34 and 1.28 kBq kg^{-1}, respectively (Table 2), which confirmed that ^{238}U was in secular equilibrium with its daughter nuclide ^{226}Ra. The U activity concentration in the debris was above the 1 Bq g^{-1} maximum limit, thus the alum shale can be considered low-level radioactive waste (FOR-2016-12-16-1659, 2016). Finally, the estimated NP and AP of 24 and 97 kg $CaCO_3$ eq t^{-1}, respectively, resulted in a ratio of 0.25. This fits well with the geochemical characterization (-Section 1.2 in the SI) which placed the debris in the 3a horizon of the alum shale formation, a horizon that is expected to be acid producing and have high concentrations of several potentially harmful trace elements and NORM (Owen et al., 1990; Pabst et al., 2017).

After AOC and LOC leaching treatments, slight or no significant changes were observed in the alum shale TIC concentrations (decreased to ~0.25 % in both treatments) or OM concentrations, nor in the mineral composition (Table 1).

Table 1
Characterization of the alum shale debris before (untreated starting material; $n = 1$) and after 52 weeks leaching under atmospheric (AOC) and low oxygen (LOC) conditions. For AOC and LOC samples, mass % are given as average ± one standard deviation of replicate samples (n = 2 except for LOI and TIC of the AOC treatment where n = 3). Amorphous and mineral phase composition in % of total mass were obtained from Rietveld simulations performed on X-ray diffractograms (further details in Section 1.3 in the SI). Size fractionation and TOC were not analysed (n.a.) in leached alum shale samples.

		Alum shale sample		
Parameter	Unit	Starting material	AOC treatment	LOC treatment
Loss on ignition (LOI)	%	13	13.1 ± 0.3	13.1 ± 0.1
Total inorganic carbon (TIC)	%	0.29	0.25 ± 0.06	0.25 ± 0.01
Total organic carbon (TOC)	%	8.9	n.a.	n.a.
Size fractionation				
Sand	%	86.6	n.a.	n.a.
Silt	%	12.2	n.a.	n.a.
Clay	%	1.2	n.a.	n.a.
Phase composition				
Muscovite	%	43.7	44.8 ± 0.4	45.8 ± 0.9
Quartz	%	19.2	19.6 ± 0.1	19.5 ± 0.9
Pyrite	%	3.5	3.9 ± 0.1	3.8 ± 0.1
Calcite	%	2.4	2.7 ± 1.2	1.8 ± 0.2
Amorphous material	%	30.9	29.0 ± 0.6	29.1 ± 0.1

3.2. Leaching experiments

3.2.1. Changes in physical-chemical variables

The redox potential (E_h) in leachates of both treatments ranged between ~250–500 mV during the experiment. The initial dissolved O_2 concentration in the artificial rainwater was 8.4 and 0.01 mg L^{-1} in the AOC and LOC systems, respectively, increasing to 9.0 and 0.2 mg L^{-1} within 1 h followed by an apparent plateau at 9.5–10.1 and 0.3–0.9 mg L^{-1} for the remaining 52-week experiment (Fig. 2a). Measurements of the gas phase (Fig. 3) showed that the oxygen levels in the LOC systems throughout the experiment (0.4–4.1 %) were substantially lower than atmospheric levels (i.e., 21 %). The P_{CO2} in the gas phase increased with time (Fig. 3), and by the end of the experiment, when the bottles had been closed for 24 weeks (i.e., gas phase had not been exchanged), observed P_{CO2} was ~5 times higher than global atmospheric CO_2 levels at 390 ppm (Hartmann et al., 2013). The methane concentrations (Fig. 3) were also higher than atmospheric levels, with an increase to 4.5 ppm already after 1 h, to ~70 ppm after 24 h, and up to 3 orders-of-magnitude higher than the ~1.8 ppm global atmospheric P_{CH4} (Hartmann et al., 2013) 1 week into the experiment.

Mixing the synthetic rainwater with the alum shale debris increased the pH from ~5.0 to 8.4 (AOC) and 9.0 (LOC) within the first hour (Fig. 2b). In the AOC leachate, the pH dropped to 7.0 at 24 h, followed by an increase to 8.0 after 4 weeks, before slowly decreasing again to 7.7 by 52 weeks. The LOC treatment showed no initial pH drop, but the slow decrease to pH 7.7 during the 52 weeks was similar to the AOC systems. Alkalinity (Fig. 2c) and conductivity (Fig. 2d) were similar in both treatments during the first 4 weeks, with a rapid increase after the initial mixing. This was followed by stabilization of alkalinity at ~1.1 mmol L^{-1} in the AOC leachates and a steady increase to 1.9 mmol L^{-1} in the LOC leachates, while conductivity increased steadily for the rest of the experiment. The conductivity was ~15 % higher in AOC than LOC leachates.

Sulphate was, together with carbonates, the dominating anion in the leachate of both treatments (Fig. 2e), increasing rapidly within 4 weeks followed by a slower rate for the rest of the experiment. Sulphate concentrations were ~ 30 % higher in the AOC than in the LOC leachates. The initial nitrate concentration in the synthetic rainwater (1.3 mg L^{-1}) decreased

Table 2
Elemental composition (average ± one standard deviation, n = 3) of untreated alum shale used in the leaching experiments, percentage of the elements leached from the alum shale into solution under atmospheric (AOC, n = 3) and low oxygen (LOC, n = 2) conditions after 52 weeks reaction, and concentration ratio of AOC and LOC treatments at week 52.

		Alum shale		AOC leachate	LOC leachate	
		Total concentration		% of rock	% of rock	AOC/LOC[a]
Group 1	Li	31.3 ± 0.3	mg kg^{-1}	0.66	0.45	1.5***
(Alkali metals)	Na	3.23 ± 0.03	g kg^{-1}	1.1	1.0	1.1
	K	42 ± 1	g kg^{-1}	0.13	0.13	1.0
Group 2	Be	6.7 ± 0.2	mg kg^{-1}	<0.0007	0.0008	†
(Alkaline earth metals)	Mg	9.0 ± 0.3	g kg^{-1}	0.94	0.85	1.1
	Ca	13 ± 5	g kg^{-1}	9.5	8.8	1.1*
	Sr	0.146 ± 0.007	g kg^{-1}	16	15	1.1
	Ba	0.8 ± 0.1	g kg^{-1}	0.02	0.03	0.73***
	^{226}Ra	35 ± 2	ng kg^{-1}	0.12	0.09	1.3
		1.28 ± 0.07	kBq kg^{-1}			
Group 4–11	V	3.08 ± 0.08	g kg^{-1}	0.0006	0.0002	3.0***
(Transition metals)	Cr	0.14 ± 0.03	g kg^{-1}	0.0001	0.0001	1.1†
	Mo	0.226 ± 0.004	g kg^{-1}	22	7.1	3.1***
	Mn	0.27 ± 0.05	g kg^{-1}	6.3	5.6	1.1*
	Fe	32 ± 3	g kg^{-1}	0.00009	0.0001	0.62*
	Co	23.4 ± 0.1	mg kg^{-1}	0.78	0.33	2.4***
	Ni	0.44 ± 0.03	g kg^{-1}	1.2	1.4	0.84*
	Cu	0.141 ± 0.005	g kg^{-1}	0.007	0.004	2.0***
Group 12	Zn	0.51 ± 0.04	g kg^{-1}	1.8	0.43	4.2***
(Zinc group)	Cd	11.2 ± 0.8	mg kg^{-1}	2.6	0.82	3.2***
Group 13 (Icosagens)	Al	79 ± 1	g kg^{-1}	0.000009	0.00003	0.35**
Group 14	Sn	3.67 ± 0.06	mg kg^{-1}	0.002	0.0008	2.2†
(Crystallogens)	Pb	47 ± 1	mg kg^{-1}	0.0004	0.0004	1.0
Group 15	P	0.81 ± 0.05	g kg^{-1}	0.0003	0.0009	0.31†
(Pnictogens)	As	88 ± 4	mg kg^{-1}	0.009	0.003	2.9***
	Sb	19.1 ± 0.8	mg kg^{-1}	0.70	1.0	0.68***
Group 16 (Chalcogens)	S	31 ± 3	g kg^{-1}	3.3	2.5	1.3**
Rare earth elements	La	50 ± 1	mg kg^{-1}	0.0001	0.0002	0.57*
Lanthanides and group 3	Ce	92 ± 2	mg kg^{-1}	0.00007	0.0002	0.36**
	Pr	12.9 ± 0.4	mg kg^{-1}	0.00009	0.0002	0.48**
	Nd	47 ± 2	mg kg^{-1}	0.0001	0.0002	0.58
	Sm	9.4 ± 0.2	mg kg^{-1}	0.0003	0.0004	0.79
	Eu	1.8 ± 0.1	mg kg^{-1}	0.001	0.001	1.1†
	Gd	9.1 ± 0.3	mg kg^{-1}	0.0007	0.0007	0.94
	Dy	8.5 ± 0.3	mg kg^{-1}	0.001	0.002	0.87
	Ho	1.88 ± 0.05	mg kg^{-1}	0.002	0.002	1.1
	Er	5.0 ± 0.2	mg kg^{-1}	0.002	0.002	1.1
	Tm	0.75 ± 0.01	mg kg^{-1}	0.002	0.003	0.83
	Yb	4.35 ± 0.04	mg kg^{-1}	0.002	0.002	1.2
	Lu	0.66 ± 0.01	mg kg^{-1}	0.002	0.002	0.99
Actinides	Th	14.8 ± 0.7	mg kg^{-1}	<0.00004	0.0002	†
	^{232}Th	0.060 ± 0.002	kBq kg^{-1}			
	U	107 ± 2	mg kg^{-1}	4.0	4.9	0.82***
	^{238}U	1.34 ± 0.02	kBq kg^{-1}			

[a] Significance levels for t-test between AOC and LOC concentrations: *$p < 0.1$, **$p < 0.05$, ***$p < 0.01$, † t-test not performed as at least one replicate was below the detection limit.

within 4 weeks to below (or within error of) the detection limit (0.09 mg L^{-1}) in both treatments (Fig. 2f), whereas the initial chloride concentration (0.46 mg L^{-1}) decreased to ~0.3 mg L^{-1} in AOC leachates while remained within error of 0.5 mg L^{-1} in the LOC leachates (Fig. 2g). Fluoride increased from <0.04 mg L^{-1} in the rainwater to 0.30–0.35 mg L^{-1} in the leachates from both treatments (Fig. 2h).

3.2.2. Element leaching development

Leached concentrations of Be, Cr, Fe, Cu, P, ^{232}Th, group 13 and 14 elements, and rare earth elements were close to or below detection limit (see Table S3 for average concentrations at week 52), thus leachate concentrations over time are not presented here. For the remaining elements, comparison of the dissolved fraction (< 0.45 μm) with the <10 kDa fraction at 1 h and 4, 12, 28 and 52 weeks showed that ≥90 % were present in the leachates as LMM species. Due to the similarities between the fractions, only results for the dissolved fraction samples are presented here.

In general, the leachate concentrations of most of these elements increased abruptly during the first hour after mixing and up to 1 week contact time, independently of the treatment (Fig. 4). This can be an artefact from crushing the alum shale, which created very reactive, fresh surfaces that could enhance the release of elements from the mineral phase. Therefore, when discussing the long-term leaching processes studied in this work, the first initial high element release (i.e., < 1 week) was not considered unless presented or discussed otherwise.

After 1 week, leached concentrations of Li under LOC and Na and K in both treatments stabilized or decreased slightly, whereas Li in the AOC systems continued to increase (Fig. 4a, b, c), reaching a 46 % higher concentration than under LOC conditions at week 52 (p = 0.0002; Table 2). Potassium concentrations (5–6 mg L^{-1}) were almost twice as high as Na concentrations (3–4 mg L^{-1}) and no significant differences were observed between treatments for either element during the experimental period. Contrastingly, leached Mg, Ca and Sr concentrations increased over time for both treatments, but at slower rates for the LOC systems (Fig. 4d, e, f). Yet, after 52 weeks, concentrations in both treatments were similar for Mg (~8 mg L^{-1}) and Sr (~2.2 mg L^{-1}), and only slightly higher in AOC than LOC for Ca (125 and 116 mg L^{-1}, respectively, p = 0.07). Concentrations of Ba and ^{226}Ra decreased over time (Fig. 4g, h), with LOC treatment resulting in a slower Ba decrease. By the end of the experiment, about half of the Ba and Ra leached in the first week had been removed from solution and thus the final concentrations were ~16–22 μg L^{-1} Ba and

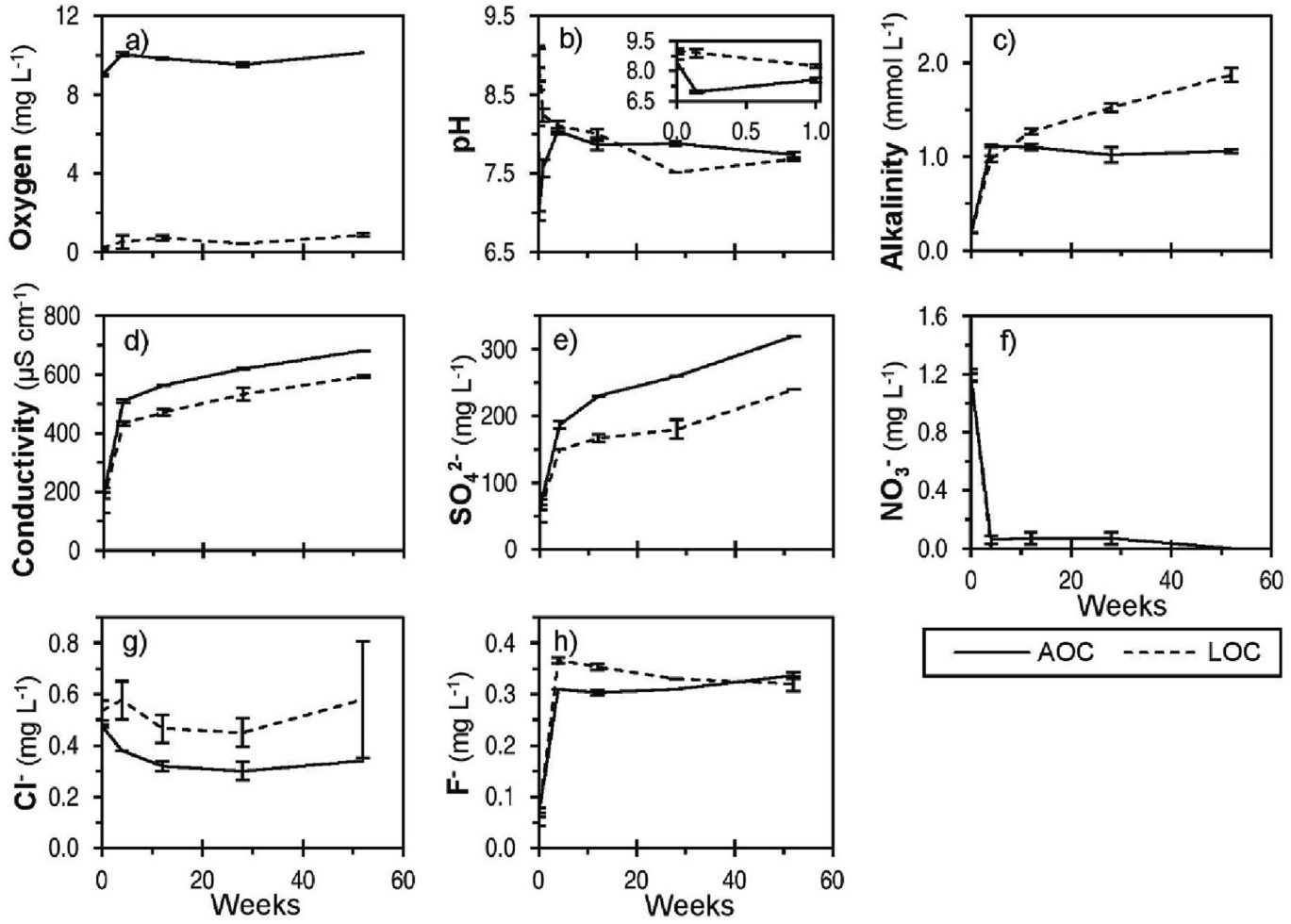

Fig. 2. Water quality parameters (a-d) and anions (e-h) in alum shale leachates of atmospheric (AOC) and low oxygen conditions (LOC) over time. Full (AOC) and dashed (LOC) lines connect average concentrations, and the error bars represent one standard deviation of replicate samples ($n = 3$, except weeks 28 and 52 for the LOC treatment where $n = 2$). The inset graph in b) shows the pH in the first week.

3.3–4.2 pg L^{-1} Ra. At week 52, Ba concentrations in leachate were 27 % lower under AOC condition than in the LOC leachates ($p = 0.003$), while the ^{226}Ra measurements were not significantly different.

The concentration of transition metals Mo, Mn, Co, and Ni increased over time with both treatments, while V decreased quickly to a 4-fold lower concentration (Fig. 4i). The AOC treatment resulted in a more rapid removal of V from solution followed by a slow increase between 12 and 52 weeks, whereas in the LOC systems the V levels remained constant after 28 weeks. By the end of the experiment, the V concentration under AOC was 3 times those reached in the LOC systems ($p = 5{\cdot}10^{-5}$). For Mo, Mn, Co, Zn and Cd (Fig. 4j, k, l, n, o), the AOC treatment resulted in faster leaching and, by week 52, the resulting concentrations were 210 % ($p = 4{\cdot}10^{-5}$), 14 % ($p = 0.07$), 140 % ($p = 0.001$), 320 % ($p = 7{\cdot}10^{-5}$), and 220 % ($p = 0.0007$) higher than under LOC, respectively. In the LOC treatment, Mo concentrations stabilized at ~1600 µg L^{-1} after 12 weeks, while the other element concentrations continue to increase. In the case of Ni (Fig. 4m), concentrations in leachate from the LOC treatment by the end of the experiment were higher than in the AOC systems (16 %; $p = 0.08$) despite that under AOC there was a faster initial release and the concentrations at week 12 were 160 % higher ($p = 9{\cdot}10^{-7}$).

Leaching of group 15 elements, that is, P (data not shown), As (Fig. 4p) and Sb (Fig. 4q), was limited and the initial concentrations decreased over time under both treatments. Antimony concentrations were ca. 20 times higher than As, with LOC resulting in 46 % higher leaching of Sb at week 52 than in AOC systems, whereas As concentrations were 66 % lower in LOC compared to AOC.

The release of ^{238}U (Fig. 4r) was initially fast (from 0 to ~200 µg L^{-1} during the first 4 weeks) followed by slower leaching, without reaching a steady-state concentration. The LOC treatment resulted in higher U concentrations in solution at week 52 than under AOC condition (529 vs. 433 µg L^{-1}), especially in the last part of the experiment with 22 % higher U at week 52 ($p = 0.001$). It is worth noting that the ^{226}Ra activity concentrations in the AOC and LOC leachates during the first 24 h were 4–8 times higher than that of ^{238}U, but by week 52 the ^{238}U activity concentrations were 36 times higher (Fig. 2 h).

3.2.3. Amount leached after 52 weeks

For most elements and for either treatment, ≤ 1 % of the total debris content had leached into the rainwater at week 52, except for Ca, Sr, Mo, Mn, Ni, Zn, Cd, S and U whose released fractions were notably higher (Table 2). Out of the total debris content, ~9 % Ca, ~6 % Mn, ~1.3 % Ni and ~3 % S leached from the alum shale under either treatment, whereas the total leached Zn and Cd was ~2–2.5 % under AOC compared to 0.4–0.8 % observed under LOC. The greatest leached fractions were obtained for Sr and Mo, with 15–16 % (AOC and LOC) and 7 % (LOC) and 22 % (AOC) of the total alum shale content released into the rainwater, respectively. In the case of radionuclides, 4.0 % and 4.9 % of the total U in the debris leached during the AOC and LOC treatments, respectively. Although the fractions of ^{226}Ra leached under AOC and LOC were 3–6 times greater than Ba, it only represented 0.12 % and 0.09 % of total ^{226}Ra debris content, respectively.

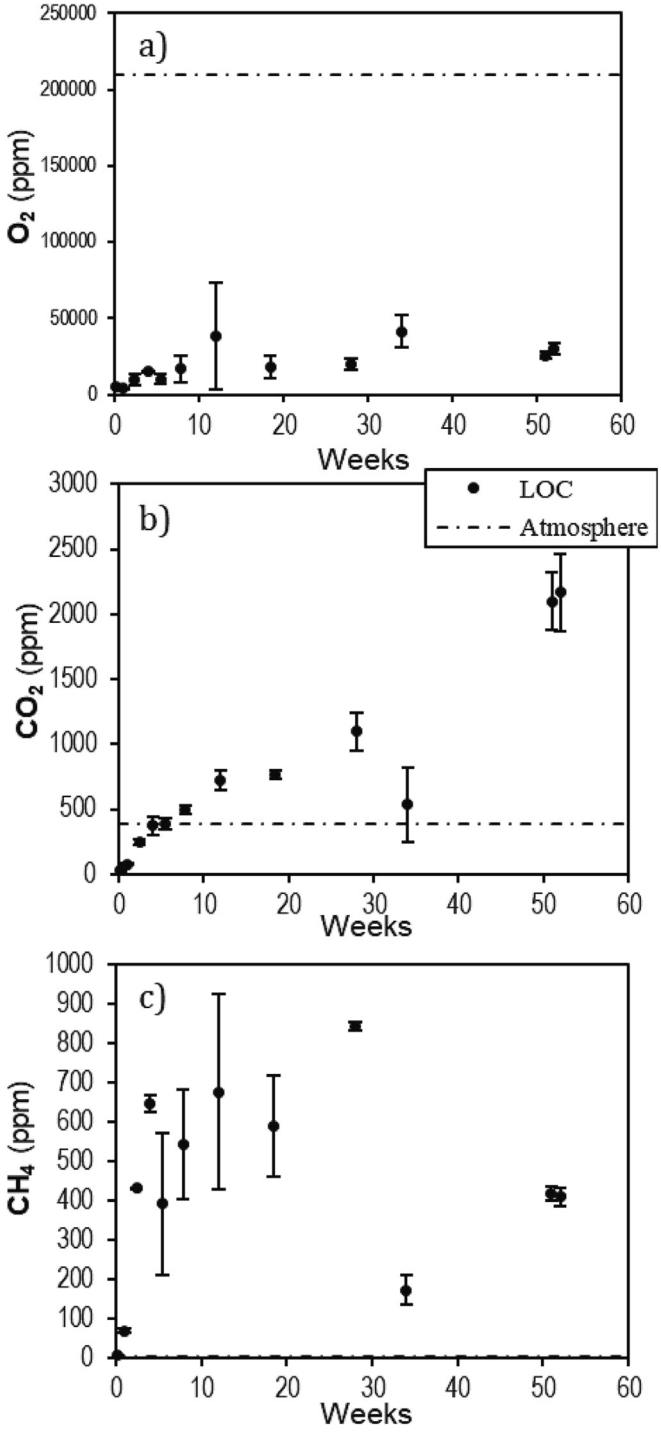

Fig. 3. Average concentrations of (a) O_2, (b) CO_2, and (c) CH_4 measured in the gas phase of alum shale samples leached under low oxygen conditions (LOC) for 52 weeks. Error bars represent one standard deviation of replicate samples (n = 3, except 28 and 52 weeks where n = 2). The atmospheric concentrations of 21 % O_2, 390 ppm CO_2, and 2 ppm CH_4 are represented by dashed lines (Hartmann et al., 2013). Note that since the gas phase was exchanged every time the rainwater was sampled (inside a nitrogen filled glove bag) the measurements do not represent a continuous time evolution.

3.3. Disposal site water

Water collected at the disposal site pond showed slightly basic pH, high conductivity (1236 μS cm^{-1}) and generally high concentrations of anions (NO_3^-, SO_4^{2-}, Cl^-) and most metals (Table 3). The concentrations of Cr, Co, Cu, Cd, Sn, Pb, and La were below 0.5 μg L^{-1}, whereas Be, Zn and Th were below the limit of detection. Uranium was the only radionuclide detected in the disposal water (73 μg L^{-1}). Phosphorus, Ba, ^{226}Ra and most rare earth elements were not measured. It is worth noting that >90 % of the detected elements were present in the disposal site water as LMM species (fractionation results reported in Wærsted (2019)).

4. Discussion

4.1. Alum shale stability under different oxygen conditions

4.1.1. Main leaching processes

The leaching of alum shale by rainwater was dominated by three main processes: pyrite oxidation, sulphate phases dissolution, and calcite dissolution. The oxidation of pyrite (FeS_2) was expected based on the measured pH (Fig. 2b) and E_h (~250–500 mV), which placed the alum shale systems in the stability range of Fe(III) (Grundl et al., 2011). The oxidation of FeS_2 by oxygen in the presence of water leading to the formation of acid (H^+), sulphates (SO_4^{2-}), and aqueous Fe(II) and Fe(III) species (Dos Santos et al., 2016) is supported by the measured release of S into the water in the form of sulphate (total S and sulphate concentrations agreed well at all time points), with concentrations increasing with time after a fast release at the beginning of the experiment (Fig. 2e). Additionally, the observed decrease in nitrate concentrations (Fig. 2f) can be explained by the use of nitrate as electron acceptor for pyrite oxidation. Although the evaluation of the leachate concentrations implied pyrite oxidation, no significant changes in pyrite concentration in the debris were observed by the end of the experiments. Since only 3.3 % of the total S leached in the AOC treatment, and a part of this likely came from dissolution of soluble sulphate phases present in the alum shale, the associated decrease of 0.1–0.2 % in the pyrite fraction would not be detectable by XRD. Overall, these results suggest that the rainwater leaching at atmospheric or low oxygen conditions used in this study was not very aggressive towards the rock. Oxygen is often the limiting factor in pyrite oxidation (Chandra and Gerson, 2010). By submerging the alum shale in water, the oxygen availability was reduced due to slower diffusion in water compared to air. Moreover, since the rate of pyrite oxidation depends on surface area (Chandra and Gerson, 2010), the relatively large grain size of the debris used in this study (<2 mm) could have limited the available reactive surfaces and thereby decreased the oxidation rate, compared to, e.g., the experiments by Jeng (1991) using smaller debris (< 75 μm).

Calcium and carbonates were the other main ions observed in the leachates and, by the end of the experiment, pH was still circumneutral (Figs. 2b, c and 3e), indicating that the release of carbonates due to dissolution of the calcite ($CaCO_3$) fraction in the debris neutralized the H^+ released from pyrite oxidation. The concentration of dissolved carbonate was limited by the solubility of calcite and, at the experimental pH of ~7.7, carbonates would mainly be present as bicarbonate (HCO_3^-), thus providing sufficient buffering capacity to maintain a circumneutral pH for 52 weeks. Other leaching experiments with alum shale from Gran have reported similar neutral pH (Fjermestad et al., 2017; Hjulstad, 2015; Waersted et al., 2020). In a 14-week weathering batch experiment using a calcareous alum shale, Jeng (1991) measured decreasing pyrite content and increasing leaching of sulphate and Ca, while no change in pH was observed due to neutralization of the acid by carbonate provided by dissolved calcite, as seen here. Nevertheless, Scandinavian alum shales can result in pH levels down to 2–3 (Falk et al., 2006; Yu et al., 2014) and the measured NP:AP of our alum shale (0.25) reflects that pH would decrease with time if conditions for oxidation are met. In laboratory scale, unsaturated columns and in large scale, outdoor batch leaching experiments with Norwegian alum shale, i.e., in systems with greater access to oxygen compared to our bottle batch experiments, the time required for the pH to drop below ~6 was ~10 months and between 14 months to 8 years, respectively (Wærsted et al., 2022). Thus, the length of our AOC/LOC experiments may have not been sufficient to observe the expected pH drop.

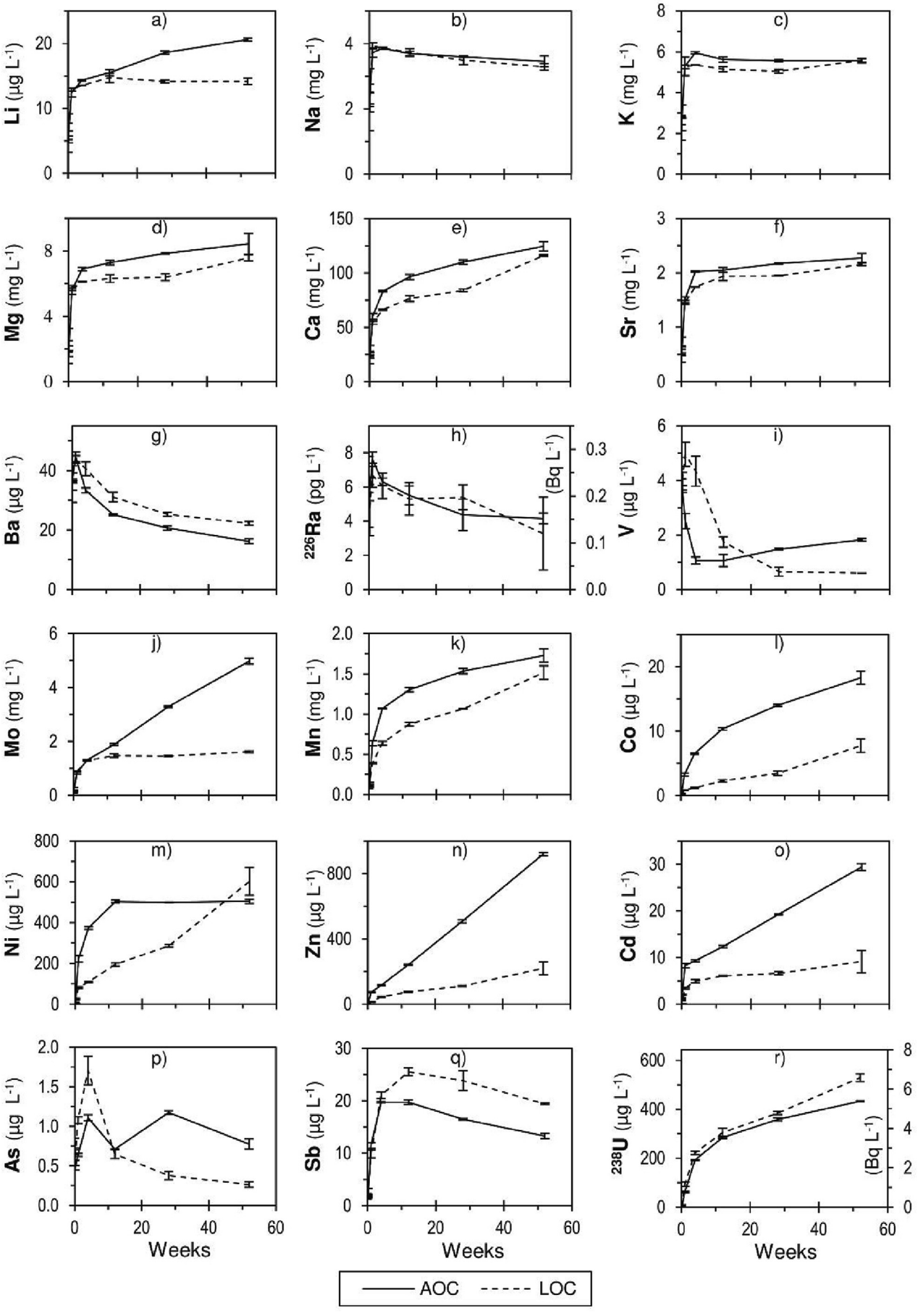
a)
Li (µg L-1)
b)
Na (mg L-1)
c)
K (mg L-1)
d)
Mg (mg L-1)
e)
Ca (mg L-1)
f)
Sr (mg L-1)
g)
Ba (µg L-1)
h)
226Ra (pg L-1)
(Bq L-1)
i)
V (µg L-1)
j)
Mo (mg L-1)
k)
Mn (mg L-1)
l)
Co (µg L-1)
m)
Ni (µg L-1)
n)
Zn (µg L-1)
o)
Cd (µg L-1)
p)
As (µg L-1)
q)
Sb (µg L-1)
r)
238U (µg L-1)
(Bq L-1)
Weeks
Weeks
Weeks
AOC
LOC

Table 3
Water quality and element concentrations measured in water collected at the disposal site at Gran (average ± one standard deviation; n = 1 for pH and conductivity, n = 3 for the rest of the measurements) and ratios to the experimental measurements obtained under atmospheric (AOC, n = 3) and low (LOC, n = 2) oxygen conditions at week 52. Concentrations were measured in samples filtered through 0.45 μm, except for field parameters, TOC and anions in disposal site water that were measured in unfiltered samples.

		Disposal site water		Concentration ratios	
		Concentration	unit	AOC/site	LOC/site
Water quality	pH	7.65		1.0	1.0
	Conductivity	1236	μS cm^{-1}	0.55	0.48
	TOC	1.5	mg L^{-1}	–	–
	SO_4^{2-}	340	mg L^{-1}	0.94	0.71
	NO_3^-	186	mg L^{-1}	≤0.0005	≤0.0005
	Cl^-	23	mg L^{-1}	0.043	0.026
Group 1	Li	20 ± 0.2	μg L^{-1}	1.0	0.71
(Alkali metals)	Na	99 ± 1	mg L^{-1}	0.035	0.033
	K	13 ± 0.1	mg L^{-1}	0.43	0.43
Group 2	Be	<0.0083	μg L^{-1}	–	–
(Alkaline earth	Mg	12 ± 0.4	mg L^{-1}	0.70	0.63
metals)	Ca	110 ± 4	mg L^{-1}	1.1	1.1
	Sr	1.40 ± 0.03	mg L^{-1}	1.6	1.5
Group 4–11	V	2.4 ± 0.06	μg L^{-1}	0.76	0.25
(Transition metals)	Cr	0.14 ± 0.03	μg L^{-1}	0.14	0.11
	Mo	850 ± 0.4	μg L^{-1}	5.9	1.9
	Mn	97 ± 2	μg L^{-1}	18	16
	Fe	4.4 ± 0.7	μg L^{-1}	0.64	1.0
	Co	0.48 ± 0.07	μg L^{-1}	38	16
	Ni	4.3 ± 0.2	μg L^{-1}	117	140
	Cu	0.26 ± 0.02	μg L^{-1}	3.8	1.9
Group 12	Zn	<2.6	μg L^{-1}	≥354	≥85
(Zinc group)	Cd	0.13 ± 0.006	μg L^{-1}	226	70
Group 13 (Icosagens)	Al	7.8 ± 0.4	μg L^{-1}	0.091	0.26
Group 14	Sn	0.12 ± 0.002	μg L^{-1}	0.058	0.025
(Crystallogens)	Pb	0.042 ± 0.0007	μg L^{-1}	0.48	0.40
Group 15	As	3.7 ± 0.07	μg L^{-1}	0.21	0.071
(Pnictogens)	Sb	90 ± 0.4	μg L^{-1}	0.15	0.22
Rare earth elements	La	0.0087 ± 0.002	μg L^{-1}	1.1	1.3
Actinides	Th	<0.004	μg L^{-1}	–	≥0.8
	U	73 ± 0.4	μg L^{-1}	5.9	7.2

In the LOC systems, the oxidation of pyrite was less pronounced than under atmospheric oxygen conditions. As indicated by the observed oxygen levels (Figs. 2a and S9a), less oxygen was available compared to the AOC systems, and thus pyrite oxidation occurred to a lesser extent in the LOC systems, leading to significantly lower leaching of sulphate (Table 2; Fig. 2e). This limited oxidation is also supported by 13 % lower conductivity (Fig. 2d), which indicated that the total ion concentration leached into the water under LOC was lower. At week 52, the LOC systems had 76 % higher alkalinity than the AOC leachates ($p = 0.0007$), which could indicate lower production of acid from pyrite oxidation. However, since the carbonate concentration in the AOC systems was limited by calcite solubility, the higher alkalinity in the LOC systems can be explained by the higher P_{CO2}, which would increase the carbonate solubility. The increase in P_{CO2} originated most likely from CO_2 released as acid was neutralized by carbonates, subsequently building up in the closed LOC bottles (gas exchange only during sampling). Since the alum shale debris was not sterilized prior to the experiments, the elevated methane concentrations observed in the gas phase (Fig. 3c) and the decrease in NO_3^- concentrations in the leachates (Fig. 2f) could suggest biological activity also occurring to some extent in these systems.

4.1.2. Release of trace elements

Changes in water quality and gas phase conditions caused by the main leaching processes (i.e., pyrite oxidation, sulphate and calcite dissolution) affected the release of elements from the alum shale differently and resulted in different associated processes. Dissolution of pyrite due to oxidation produced aqueous Fe(III), which at the experimental pH would precipitate as amorphous oxyhydroxide, $Fe(OH)_3$, and lead to scavenging of a variety of trace elements from solution (Braunschweig et al., 2013). In this study, Fe concentration in the leachates were close to or below detection limit and a sudden pH drop from 8.4 to 7.0 was observed within 24 h in the AOC systems (Fig. 2b), which suggested that the initial Fe released from pyrite oxidation rapidly precipitated, removing OH^- from solution to form $Fe(OH)_3$. These amorphous iron precipitates have a high affinity for elements such as V, As and Sb (Braunschweig et al., 2013; Okkenhaug, 2012), which can occur as impurities in pyrite and thus being released during the leaching process. In the rainwater leaching experiments, the V, As and Sb leachate concentrations were relatively low and/or decreased over time (Fig. 4i, p, q), likely due to scavenging by the iron phases concurrently formed during the experimental period (pH of the leachates was >6.9; Fig. 2b). In the LOC systems, where the pyrite oxidation was limited (i.e., less Fe released into solution), the lack of the initial pH drop and the slower decrease in V, As and Sb concentrations in the leachate compared to the AOC systems (Figs. 2b and 4i, p, q) suggested that element scavenging by $Fe(OH)_3$ was a less dominant process.

The fast release of K during the first 4 weeks (Fig. 4c) could be an artefact due to the crushing process, but the slightly higher concentrations in the leachate from the AOC treatment (except at week 52 when the two treatments had equal concentrations) indicates an oxidation effect. This same effect has also been observed by Waersted et al. (2020) in alum shale leaching experiments at neutral pH. Of the other alkali metals, Na leaching was the same for both treatments, while for Li there was a clear effect of the oxygen access. Muscovite accounts for all the K in the debris and can be the source of the released fluoride (Fig. 2h). Dissolution of muscovite would also release Al. However, the Al concentrations in the leachates were below the detection limit, suggesting that the Al solubility in these systems was controlled by the formation of amorphous $Al(OH)_3$, as seen in long-term weathering of black shale at pH > 6 (Yu et al., 2014).

Precipitation and/or co-precipitation likely limited the solubility of the heavy alkaline earth metals Ba and ^{226}Ra as only ≤0.12 % of the total debris content was in solution at the end of the experiment (Fig. 4g, h; Table 2). Due to high sulphate concentrations, the leachates at all sampling points were slightly oversaturated with respect to $BaSO_4$ ($K_{sp} = 1.07{\cdot}10^{-10}$, 25 °C; (CRC, 1993)), suggesting that the released Ba precipitated as $BaSO_4$ (Ba concentrations decreased over time, while SO_4^{2-} concentration increased; Figs. 2e and 4g). Since the concentrations of ^{226}Ra (Fig. 4h) followed a very similar trend to Ba, Ra was likely co-precipitated with $BaSO_4$. This Ba/^{226}Ra (co-)precipitation process was supported by the higher Ba leachate concentrations observed in the LOC systems, where the release of sulphate was lower compared to the AOC treatment.

The more pronounced pyrite oxidation under the atmospheric oxygen conditions compared to the LOC corresponded well with the significantly greater release of Mo, Co, Zn Cd, and initially of Ni (Fig. 4; Table 2), which are commonly found as impurities in pyrite and can be released during leaching in acidic conditions (Abraitis et al., 2004; Yu et al., 2014). The difference between treatments was especially noticeable for Mo, Zn and Cd (Fig. 4j, n, o) and to a lesser extent Co (Fig. 4l). The concentrations in the LOC systems reached an apparent steady state during the experimental period compared to the linear increase observed under AOC, which resulted in 2–4 times higher leachate concentrations at week 52 (Table 2). These observations are in accordance with the high release of Mo reported for alum shale from Gran (Fjermestad et al., 2017; Hjulstad, 2015; Santos, 2014) and for other alum shales (Lavergren et al., 2009), as well as with the Cd

Fig. 4. Dissolved (< 0.45 μm) concentrations of selected elements in alum shale leachates under atmospheric (AOC) and low oxygen (LOC) conditions over time. Full (AOC) and dashed (LOC) lines connect average concentrations, and error bars represent one standard deviation of replicate samples (n = 3, except weeks 28 and 52 of LOC treatment where n = 2). For the radionuclides (h and r), the secondary y-axis shows activity concentrations (Bq L^{-1}).

concentrations reported for large-scale experiments with Gran alum shale left open to air over 8 months (~18 μg L^{-1} after 32 weeks (Fjermestad et al., 2017) vs. ~20 μg L^{-1} at 28 weeks in the AOC leachates (Fig. 4o)). Leached Cd concentrations reported for shorter reaction times were ca. 1 order-of-magnitude lower than those observed here under the AOC after similar leaching time (i.e., ~0.5 μg L^{-1} (Hjulstad, 2015) vs. ~10 μg L^{-1} (Fig. 4o) after 4 weeks), likely due to differences in particle size and heterogeneity of the rock. In the case of Ni (Fig. 4m), a steady-state release was observed in the AOC systems after 12 weeks reaction, suggesting that an apparent equilibrium between Ni-containing phases and Ni aqueous species in the rainwater was reached. However, no equilibrium was reached under the LOC, as Ni leachate concentrations continued to increase over time.

The release of major cations (Mg, Ca), Sr and Mn (Fig. 4d, e, f, k) resembled that of SO_4^{2-} (Fig. 2e), which suggests that the dissolution of calcite to buffer the acid produced during pyrite oxidation released Ca into solution as well as other doubly-charged cations that can be present as impurities in carbonate phases (Gabitov et al., 2013). Since the total amount leached from the debris by the end of the experiment was higher for Ca (~9 %) than for Mg (<1 %) or Mn (~6 %) (Table 2), the latter two could also have been present as impurities of aluminosilicate phases (such as muscovite or albite) and/or forming the mineral structure of other minor phases (undetected by XRD) that were seemingly stable under both leaching conditions of this study. The initial total concentration of Sr in the debris was 2 orders-of-magnitude lower than Ca (Table 2), supporting the potential substitution of Ca by Sr in the structure of calcite or other minor phases. Yet, the fraction leached by the end of the experiment was higher for Sr than Ca (~15 % vs. ~9 %). This suggests that the release of Sr was not only due to calcite dissolution (otherwise stoichiometric or lower release expected), but could also have been driven by cation exchange (Perdrial et al., 2014), i.e., Sr in the mineral structure was replaced by other cations present in the aqueous phase. It is worth noting that, although the release of Mg, Ca, Sr or Mn did not plateau at week 52, limited access to oxygen significantly diminished the leaching rates from week 4 onwards (LOC systems; Fig. 4d, e, f, k). This agrees with the observed lower production of acid from pyrite oxidation and the consequent lower requirement for buffering in the LOC systems compared to the AOC systems.

The mobility of ^{238}U from alum shale due to rainwater immersion was greater than that observed for other radionuclides (i.e., 0.0002 % or less for ^{232}Th and ~ 0.1 % of the ^{226}Ra leached from the debris; Table 2) but in agreement with previous open air leaching studies using Gran alum shale with characteristics similar to the debris used here. The U leachate concentrations (i.e, ~400–500 μg U L^{-1} at 28–52 weeks; Fig. 4r) were within range of those reported after 4–7 weeks reaction time (~100–350 μg L^{-1}) and ca. half of those after 8 months (~1100 μg U L^{-1}) (Fjermestad et al., 2017; Hjulstad, 2015). Besides the particle size of the debris and the initial properties of the leachant, these leaching differences can be attributed to variations and uneven distribution of total U concentration in the debris, even in rock materials from the same area. Uranium concentrations of the debris used here were similar to other materials extracted from the tunnel construction (Fjermestad et al., 2017), but were about 3 times higher than those reported for black shale substrates collected at different depths near Gran (Helmers, 2013). Additionally, the U release trend was not comparable to any of the other leached trace elements. Hence, these results suggest that leached U might have originated from different phases in the debris, e.g., associated with high-density inclusions in the rock heterogeneously distributed in the geological horizons of the Gran area (Skipperud et al., 2016). The total U leached at pH 7–8 and atmospheric oxygen has ranged from 1 to 10 % of the U rock content (this study and Fjermestad et al. (2017); Helmers (2013)).

Interestingly, the increasing U concentrations in the LOC leachates over the 52-week reaction period were higher than those observed under AOC (Fig. 4r). This enhanced release can be explained by: i) reduced pyrite oxidation and Fe concentrations in the LOC system causing less U scavenging by Fe (and Al) amorphous oxyhydroxides and/or ii) complexation of U by dissolved carbonate, originating from the dissolution of calcite. In the absence of scavenging phases with high affinity for U (Braunschweig et al., 2013) or high concentrations of dissolved phosphate that can readily form recalcitrant uranyl phosphate minerals (Perdrial et al., 2018; Vázquez-Ortega et al., 2021), the formation of binary and ternary uranyl carbonate complexes have been shown to increase the solubility (Stanley and Wilkin, 2019) and accelerate the dissolution rates of different uranyl mineral types (Reinoso-Maset et al., 2020; Reinoso-Maset et al., 2017). Therefore, the release of U from the alum shale debris under limited oxygen access might have been driven by carbonate complexation since lower buffering was required and P_{CO2} was higher in the low oxygen systems than under atmospheric oxygen conditions.

4.2. Leaching at the disposal site

The disposal site water collected after 60 weeks of disposing tunnel materials in the excavated bog was comparable to the 52-week alum shale leachates with respect to pH and concentrations of SO_4^{2-} and major cations such as K, Ca, Mg and Sr (Table 3;Figs. 2, 4), as well as to the size fractionation of a series of elements (Wærsted, 2019). These results indicate that weathering of the alum shale occurred on site in a similar manner to that observed in the laboratory leaching experiments. In both scenarios, laboratory and disposal site, non-weathered black shale was used (i.e., blasted rock was transported directly from the tunnel to disposal in the bog); yet, if weathered acid-producing rock were to be stored, oxidation processes could have continued even without oxygen due to Fe(III) acting as oxidant and, in turn, avoiding future acid rock drainage can become difficult (Dublet-Adli et al., 2021).

The conductivity of the disposal site water was, however, twice as high as in the leachates, which can be linked to the markedly higher concentrations of NO_3^- (> 2000 times) and Cl^- and Na (20–40 times) compared to those observed in the AOC or LOC systems (Table 3). The Na and Cl^- likely originated from salting of roads in the area, whereas the extremely high NO_3^- concentrations can be related to explosive residues found in the disposed tunnel blast materials (Fjermestad et al., 2018). Three years after the in-situ sampling, the NO_3^- concentration in the water of the finalized, covered disposal site was reported to be 0.6 mg L^{-1} (Greipsland et al., 2019), i.e., ca. 300 times lower. This decrease is in line with the rate observed in the laboratory experiments, where the leachate nitrate levels decreased at least a factor of 60 in 1 year (from 1.2 to <0.02 mg L^{-1} NO_3^-; Fig. 2). Thus, under limited water exchange at the disposal site and based on the main leaching processes observed in the AOC and LOC systems, these results imply that the nitrate was consumed mostly during the oxidation of pyrite but could also have been consumed by biological processes. Yet, the concentrations of some of the leached elements suggested that pyrite oxidation might have occurred to a lesser extent at the disposal site (Table 3): i) the ~6 to 350 times lower concentrations of Mo, Mn, Co, Ni, Zn, Cd and U in the disposal site can indicate less release from pyrite oxidation and calcite dissolution and ii) ~1.5 to 14 times higher concentrations of Li, V, As and Sb in the disposal site water could be explained by limited Fe/Al (oxy)hydroxides scavenging. These effects are likely due to limited access to oxygen as observed between the AOC and LOC leaching experiments (Table 2). The differences in leached U and other elements can also be explained by differences in the rock materials accumulated at the disposal site (i.e., black shales mixed with other rocks) and those used for the leaching experiments (i.e., alum shale debris selectively collected based on high U content). On the other hand, the release of other elements, such as Be, Cr, Fe, Cu, Al, Sn, Pb, La and Th, into disposal site pond water was low, just as observed in the laboratory leachates (Table 3) and, based on the comparable sulphate levels, the same low solubility was expected for Ba and ^{226}Ra (not measured in the disposal site water).

The buffering capacity of the disposal site water changed over time. The alkalinity reported for the disposal site at the time of our water sampling, i.e., after ca. 1.2 years of accumulating tunnel materials in the bog, was similar to the AOC leachates at week 52 (~1.4 mmol L^{-1} (Fjermestad et al., 2018) vs. ~1.1 mmol L^{-1}). After the site was covered, the alkalinity increased to up to 5–7 mmol L^{-1} over a 2 year period (Fjermestad et al.,

2018), which resembled well the increase in alkalinity observed in the LOC systems (up to ~2 mmol L^{-1} in 1 year). As seen in the laboratory experiments (Fig. 2), the pH of the disposal site water during and after accumulation of materials did not significantly decrease over time and stayed at pH 7.5–8. Thus, the buffering capacity of the rock masses was sufficient to neutralize any acid released from pyrite oxidation during storage in open air, similarly to the AOC systems. Since the water of the bog was exchanged during the filling period, dissolved carbonate could have been removed from the system leading to a reduction of buffering capacity, as reported for laboratory experiments by Waersted et al. (2020). Once the materials were covered and access to oxygen was limited, the buffering capacity in the form of carbonate alkalinity increased due to increased P_{CO2} underground, similarly to the LOC systems. P_{CO2} is commonly higher underground due to biological activity and slow exchange with the atmosphere, and in this case, CO_2 will also be released from acid neutralization by carbonates.

As the disposal site is an excavated bog, the presence of organic matter in solid and dissolved phases can play an important role in changing the speciation of elements with a high affinity for OM. In fact, TOC was observed in the disposal site water (Table 3) and fell within the reported values of 0.5–11 mg L^{-1} (Fjermestad et al., 2018). Comparison with laboratory data is difficult as these were based on filtered samples (DOC), and all were below the detection limit (1.8 mg L^{-1}). However, the role of OM is expected to have been more important at the disposal site than in the laboratory experiments. While association to TOC in water can increase the mobility of trace elements, association with solid phase OM can also reduce mobility.

5. Environmental implications of storing acid-producing rock

While the concentrations of elements of environmental concern, such as Mo, Ni, Zn, Cd and U, leached into rainwater after 52 weeks (AOC and LOC experiments) surpassed up to 300 times those reported for international environmental limits (Table 4), they were still orders of magnitude lower than those expected from alum shale drainage by low pH (Åhlgren et al., 2021; Falk et al., 2006; Jeng, 1991; Lavergren et al., 2009; Yu et al., 2014). The concentrations of Mo, Ni, Cd, As and U in the disposal site water were also above the regulative limits (Table 4), thus releases from the disposal site pond into the groundwater, eventually reaching main water streams, could increase the contamination to levels of environmental concern. Yet, the water quality of the downstream Vigga River has been reported to be within acceptable quality limits for Cr, Ni, Cu, Cd, Pb, As and U (Engebretsen et al., 2020), indicating that run-off of leachate water from the established alum shale waste disposal site so far has not been significant or that the environmental dilution is sufficient to diminish any potential pollutant accumulation.

Since the majority of the elements observed in the laboratory leachates and in the disposal site water can be assumed bioavailable (> 90 % present as LMM species), dilution of this contaminated, metal-rich water originating from alum shale leaching will reduce negative effects on biota. Field investigations have shown that there were negative effects on benthic macroinvertebrate communities in the vicinity of the disposal site during construction work (Engelstad, 2016), but uptake of elements present in alum shale from Gran, such as Mo, Cd or U, resulted in no clear toxic effects on *Salmo trutta* (Hjulstad, 2015; Skipperud et al., 2016). Higher element uptake and associated toxic effects on fish are, however, expected at low pH (Lydersen et al., 2002), thus a potential drop from pH 7.9–8.7 recorded in streams and lakes around the disposal site at Gran (Skipperud et al., 2016) would increase the environmental risk of the alum shale storage. Even if dilution may help reducing the risk, limiting infiltration of oxygen-rich water into the disposal site would be crucial to avoid the development of acid rock drainage with the associated low pH and high levels of elements of concern.

The present 52-week rainwater leaching experiments showed that, even under neutral rock drainage, alum shale can release NORM and other harmful elements at levels of concern, and that the rainwater-alum shale systems were still undersaturated with respect to several elements (no steady state reached, low total % leached). In addition, the release of most elements was lower and slower under low oxygen conditions since the pyrite oxidation was less prominent compared to atmospheric conditions, confirming the importance of storage with limited access to oxygen (e.g., anaerobic or anoxic conditions). The inherent buffering capacity of the rock corrected the initial pH drop observed in the AOC systems and avoided acid rock drainage for 52 weeks. However, in the long term, the stability of the stored alum shale can be compromised since a pH drop is expected if oxygen is available (0.25 NP:AP for the alum shale debris from Gran). These results demonstrated that when acid-producing rock is stored submerged in water, a pH drop can be avoided or postponed by minimizing the access to air and exchange of water. This is essential at the disposal site to avoid leaching of several environmentally relevant elements and the associated negative effects on biota. Moreover, for accurate environmental assessments, specific evaluation of the properties of both the disposal site (e.g., geological setting, hydrology) and rock masses (e.g., mineral and elemental composition, particle size, weathering degree, fissility) is recommended to ensure proper storage conditions of potentially acid-producing waste rock materials.

Table 4
Concentration limits for selected elements from environmental quality standards of Norway (NO), European Union (EU) and Canada (CA), and concentration ratios for the leachates under atmospheric (AOC) and low oxygen (LOC) conditions at week 52 and the disposal site water with respect to the quality standards. Ratios highlighted in bold indicate elements in a concentration exceeding the environmental quality standard by at least 1 order-of-magnitude.

Element	Environmental quality standards[a]		Concentration ratios		
	Limit (μg L^{-1})	Country	AOC/limit	LOC/limit	Disposal site/limit
Cr	3.4	NO	0.006	0.005	0.04
Mo	73	CA	**68**	**22**	**12**
Ni	4	NO + EU	**126**	**150**	1.1
Cu	7.8	NO	0.1	0.1	0.03
Zn	11	NO	**83**	**20**	<0.23
Cd[b]	0.09	NO + EU	**322**	**102**	1.4
Pb	1.2	NO	0.02	0.01	0.04
As	0.5	NO	1.6	0.5	7.4
^{238}U	15	CA	**29**	**35**	4.9

[a] Annual average environmental quality standard (AA-EQS) values for Norway (Norwegian Environmental Agency, 2016) and the European Union (EU, 2013), and long-term concentration from water quality guidelines for protection of aquatic life for Canada (Canadian Council of Ministers of the Environment, 2018).
[b] Limit for Cd depends on measured $CaCO_3$ concentrations.

CRediT authorship contribution statement

Frøydis Meen Wærsted: Conceptualization, Methodology, Investigation, Data curation, Formal analysis, Visualization, Validation, Writing – original draft, Writing – review & editing. **Estela Reinoso-Maset:** Formal analysis, Visualization, Validation, Writing – original draft, Writing – review & editing. **Brit Salbu:** Supervision, Writing – review & editing. **Lindis Skipperud:** Funding acquisition, Project administration, Supervision, Writing – review & editing.

Data availability

Data will be made available on request.

Declaration of competing interest

The authors declare that they have no known competing financial interests or personal relationships that could have appeared to influence the work reported in this paper.

Acknowledgements

This study has been funded by the Norwegian Public Road Administration through the NORWAT (Nordic Road Water) programme and by the Norwegian Research Council through its Centre of Excellence (CoE) funding scheme (Project 223268/F50).

Appendix A. Supplementary data

Synthetic rainwater composition; geochemical characterization of the alum shale debris; X-ray diffractograms of alum shale debris before and after leaching and associated Rietveld quantification results; E_h measurements; element concentrations in leachates at 52 weeks. Supplementary data to this article can be found online at doi:10.1016/j.scitotenv.2023.163035.

References

Aas, W., Platt, S., Solberg, S., Yttri, K.E., 2015. Monitoring of long-range transported air pollutants in Norway, annual report 2014. Enviromental Monitoring - M-367/2015. NILU – Norsk institutt for luftforskning [Norwegian Institute for Air Research], Kjeller, p. 109.

Abraitis, P.K., Pattrick, R.A.D., Vaughan, D.J., 2004. Variations in the compositional, textural and electrical properties of natural pyrite: a review. Int. J. Miner. Process. 74, 41–59.

Åhlgren, K., Sjöberg, V., Allard, B., Bäckström, M., 2021. Groundwater chemistry affected by trace elements (As, Mo, Ni, U and V) from a burning alum shale waste deposit, Kvarntorp, Sweden. Environmental Science and Pollution Research 28, 30219–30241.

Braunschweig, J., Bosch, J., Meckenstock, R.U., 2013. Iron oxide nanoparticles in geomicrobiology: from biogeochemistry to bioremediation. New Biotechnol. 30, 793–802.

Canadian Council of Ministers of the Environment, 2018. Water Quality Guidelines for the Protection of Aquatic Life. .. (Accessed 25 June 2019). .

Chandra, A.P., Gerson, A.R., 2010. The mechanisms of pyrite oxidation and leaching: a fundamental perspective. Surf. Sci. Rep. 65, 293–315.

CRC, 1993. Handbook of Chemistry and Physics. CRC Press, U.S.A.

Dos Santos, E.C., de Mendonça Silva, J.C., Duarte, H.A., 2016. Pyrite oxidation mechanism by oxygen in aqueous medium. J. Phys. Chem. C 120, 2760–2768.

Dublet-Adli, G., Pabst, T., Okkenhaug, G., Sætre, C., Vårheim, A.M., Tvedten, M.K., Gelena, S.K., Smebye, A.B., Kvennås, M., Breedveld, G.D., 2021. Valorisation of partially oxidized tailings in a cover system to reclaim an old acid generating mine site. Minerals 11, 987.

Engebretsen, A., Skrutvold, J., Roseth, R., 2020. Rv. 4 Gran grense - Jaren. Etterundersøkelser av vannkjemi i grunnvann og resipienter 2017-2020. Norwegian. Rv. 4 Gran grense - Jaren. Follow-up Studies of Water Chemistry in Groundwater and Recipients 2017-2020]. NIBIO-rapport. 6. Divisjon for miljø og naturressurser, Norsk Institutt for Bioøkonomi, Ås, p. 144.

Engelstad, J., 2016. Ecological Implications of Road Construction in an Alum Shale Bedrock Area: A State Highway (Rv4) Case Study. Department of Ecology and Natural Resource Management. Norwegian University of Life Sciences, Ås, p. 98 MSc.

EU (2013). Directive 2013/39/EU of the european parliament and of the council.

Falk, H., Lavergren, U., Bergbäck, B., 2006. Metal mobility in alum shale from Öland, Sweden. J. Geochem. Explor. 90, 157–165.

Fjermestad, H., Hagelia, P., Thomassen, T., 2017. Utlekkingsforsøk med svartskifer fra Rv. 4, Hadeland. Norwegian. Large-scale leaching experiment with black shale from National Road 4, Hadeland]. Statens vegvesens rapporter - Nr. 665. Statens vegvesen [Norwegian Public Roads Administration], Lillehammer, p. 68.

Fjermestad, H., Gundersen, E., Hagelia, P., Moen, A.B., Torp, M., 2018. Rv. 4 på Gran, nyttiggjering av svartskifer: sluttrapport og erfaringar. Norwegian. National Road 4 at Gran, Utilization of Black Shale: Final Report and Experiences Gathered. Statens vegvesens rapporter / NPRA reports, Oslo, p. 564.

FOR-2016-12-16-1659, 2016. Strålevernsforskriften [In Norwegian. Radiation Protection Act]. FOR-2016-12-16-1659. Helse- og omsorgsdepartementet [Ministry of Health and Care Services of Norway], Oslo.

Gabitov, R.I., Gagnon, A.C., Guan, Y., Eiler, J.M., Adkins, J.F., 2013. Accurate Mg/Ca, Sr/Ca, and Ba/Ca ratio measurements in carbonates by SIMS and NanoSIMS and an assessment of heterogeneity in common calcium carbonate standards. Chem. Geol. 356, 94–108.

Greipsland, I., Skrutvold, J., Roseth, R., 2019. Rv.4 Gran - Jaren. Etterundersøkelser av vannkjemi i grunnvann og resipienter [In Norwegian. National Road 4 Gran - Jaren. Follow-up investigations of water chemistry in groundwater and recipients]. NIBIO Rapport. 5, p. 167 Nr. 34. 5, Ås.

Grundl, T.J., Haderlein, S., Nurmi, J.T., Tratnyek, P.G., 2011. Introduction to aquatic redox chemistry. Aquatic Redox Chemistry. ACS Symposium Series. 1071. American Chemical Society, pp. 1–14.

Hartmann, D.L., AMG, Klein Tank, Rusticucci, M., Alexander, L.V., Brönnimann, S., Charabi, Y., Dentener, F.J., Dlugokencky, E.J., Easterling, D.R., Kaplan, A., Soden, B.J., Thorne, P.W., Wild, M., Zhai, P.M., 2013. Observations: atmosphere and surface. In: Stocker, T.F., Qin, D., Plattner, G.-K., Tignor, M., Allen, S.K., Boschung, J., Nauels, A., Xia, Y., Bex, V., Midgley, P.M. (Eds.), Climate Change 2013: The Physical Science Basis. Contribution of Working Group I to the Fifth Assessment Report of the Intergovernmental Panel on Climate Change. Cambridge University Press, Cambridge, United Kingdom and New York, NY, USA, p. 96.

Helmers, T.A., 2013. The Mobility of Uranium From U-containing Bedrock Materials as a Function of pH: Implications for Tunnel Construction. Department of Plant and Environmental Sciences. Norwegian Univerisyt of Life Sciences, Ås, p. 88 MSc.

Hindar, A., Nordstrom, D.K., 2015. Effects and quantification of acid runoff from sulfide-bearing rock deposited during construction of Highway E18, Norway. Applied Geochemistry 62, 150–163.

Hjulstad, M., 2015. Leaching, Uptake and Effects in Brown Trout (Salmo trutta) of Radionuclides and Metals From Black Shales and Sulphur Bearing Gneiss Department of Environmental Science. Norwegian University of Life Sciences, Ås, Norway, p. 76 MSc.

IAEA, 2014. The environmental behaviour of radium: revised edition. Technical Report Series No. 476. International Atomic Energy Agency, Vienna, p. 276.

Jeng, A.S., 1991. Weathering of some Norwegian alum shales. I. Laboratory simulations to study acid generation and the release of sulfate and metal cations (calcium, magnesium, and potassium). Acta Agric. Scand. 41, 13–35.

Jeng, A.S., 1992. Weathering of some Norwegian alum shales, II. Laboratory simulations to study the influence of aging, acidification and liming on heavy metal release. Acta Agric. Scand. Sect. B Soil Plant Sci. 42, 76–87.

Landa, E.R., 2007. Naturally occurring radionuclides from industrial sources: characteristics and fate in the environment. In: George, S. (Ed.), Radioactivity in the Terrestrial Environment. 10. Elsevier, pp. 211–237.

Lavergren, U., Åström, M.E., Falk, H., Bergbäck, B., 2009. Metal dispersion in groundwater in an area with natural and processed black shale – Nationwide perspective and comparison with acid sulfate soils. Appl. Geochem. 24, 359–369.

Lawrence, R.W., Wang, Y., 1996. Determination of neutralization potential for acid rock drainage prediction. Mining and Mineral Process Engineering. University of British Columbia, Vancouver B.C.

Lydersen, E., Löfgren, S., Arnesen, R.T., 2002. Metals in scandinavian surface waters: effects of acidification, liming, and potential reacidification. Crit. Rev. Environ. Sci. Technol. 32, 73–295.

Moulin, V., Amekraz, B., Barre, N., Planque, G., Mercier, F., Reiller, P., Moulin, C., 2004. The role of humic substances in trace element mobility in natural environments and applications to radionuclides. In: Ghabbour, E.A., Davies, G. (Eds.), Humic Substances: Nature's Most Versatile Materials. Taylor & Francis, pp. 275–286.

Norwegian Environmental Agency (2016). Quality standards for water, sediment and biota (M-608).

Okkenhaug, G., 2012. Mobility and Solubility of Antimony (Sb) in the Environment. Department of Plant and Environmental Sciences. Norwegian University of Life Sciences, Ås PhD.

Owen, A.W., Bruton, D.L., Bockelie, J.F., Bockelie, T.G., 1990. The Ordovician successions of the Oslo Region, Norway. In: Roberts, D. (Ed.), Special Publication 4. Norges Geologiske Undersøkelse (Geological Survey of Norway), Trondheim, p. 54.

Pabst, T., Sørmo, E., Endre, E., 2017. Geochemical characterisation of norwegian cambro-ordovician black mudrocks for building and construction use. Bull. Eng. Geol. Environ. 76, 1577–1592.

Perdrial, N., Thompson, A., O'Day, P.A., Steefel, C.I., Chorover, J., 2014. Mineral transformation controls speciation and pore-fluid transmission of contaminants in waste-weathered Hanford sediments. Geochim. Cosmochim. Acta 141, 487–507.

Perdrial, N., Vázquez-Ortega, A., Wang, G., Kanematsu, M., Mueller, K.T., Um, W., Steefel, C.I., O'Day, P.A., Chorover, J., 2018. Uranium speciation in acid waste-weathered sediments: the role of aging and phosphate amendments. Appl. Geochem. 89, 109–120.

Reinoso-Maset, E., Steefel, C.I., Um, W., Chorover, J., O'Day, P.A., 2017. Rates and mechanisms of uranyl oxyhydroxide mineral dissolution. Geochim. Cosmochim. Acta 207, 298–321.

Reinoso-Maset, E., Perdrial, N., Steefel, C.I., Um, W., Chorover, J., O'Day, P.A., 2020. Dissolved carbonate and pH control the dissolution of uranyl phosphate minerals in flow-through porous media. Environ. Sci. Technol. 54, 6031–6042.

Santos, S.H., 2014. Potential Mobility of Radionuclides and Trace Elements in Bedrock Materials and in the Deposition Area at a Tunnel Construction Site RV4 Gran, Hadeland. Faculty of Environmental Science and Technology. Norwegian University of Life Sciences, Ås, p. 127 MSc.

Singer, P.C., Stumm, W., 1970. Acidic mine drainage: the rate-determining step. Science 167, 1121–1123.

Skipperud, L., Alvarenga, E., Lind, O.C., Teien, H.-C., Tollefsen, K.E., Salbu, B., Wærsted, F.M., 2016. Inngrep i områder med sulfidrike mineraler: Effekter og miljørisiko [In Norwegian. Construction works in areas with sulphide containing rock. Case: Effects and Environmental Risks Related to Alum Shale Disposal Site]. Statens vegvesens rapporter - Nr. 651. Statens vegvesen [Norwegian Public Roads Administration], Oslo, p. 107.

Stanley, D.M., Wilkin, R.T., 2019. Solution equilibria of uranyl minerals: role of the common groundwater ions calcium and carbonate. J. Hazard. Mater. 377, 315–320.

vanLoon, G.W., Duffy, S.J., 2011. Environmental Chemistry - A Global Perspective. Oxford University Press, New York.

Vázquez-Ortega, A., Perdrial, N., Reinoso-Maset, E., Root, R.A., O'Day, P.A., Chorover, J., 2021. Phosphate controls uranium release from acidic waste-weathered Hanford sediments. J. Hazard. Mater. 416, 126240.

Vriens, B., Skierszkan, E.K., St-Arnault, M., Salzsauler, K., Aranda, C., Mayer, K.U., Beckie, R.D., 2019. Mobilization of Metal(oid) oxyanions through circumneutral mine waste-rock drainage. ACS Omega 4, 10205–10215.

Wærsted, F.M., 2019. Mobility of Naturally Occurring Radionuclides and Stable Elements in Alum Shale: A Case Study of Gran, Highway 4, Norway. Faculty of Environmental Sciences and Natural Resource Management. Norwegian University of Life Sciences, Ås PhD.

Wærsted, F.M., Jensen, K.A., Reinoso-Maset, E., Skipperud, L., 2018. High throughput, direct determination of 226Ra in water and digested geological samples. Anal. Chem. 90, 12246–12252.

Waersted, F.M., Riss, P.J., Skipperud, L., 2020. The effect of water exchange on the leaching of alum shale. Appl. Geochem. 119, 104610.

Wærsted, F.M., Fjermestad, H., Totland, C., Børresen, M., Slinde, G.A., Hansen, C.B., Tønnessen, E., Hagelia, P., Erstad, L., Baardvik, G., 2022. Utfordringer med svarte leirskifere: mellomlagring og naturlige blandmasser. Norwegian. Challenges With Black Shale: Temporary Storage and Naturally Mixed Masses. 2022. Fjellspregningskonferansen, Oslo.

Yu, C., Lavergren, U., Peltola, P., Drake, H., Bergbäck, B., Åström, M.E., 2014. Retention and transport of arsenic, uranium and nickel in a black shale setting revealed by a long-term humidity cell test and sequential chemical extractions. Chem. Geol. 363, 134–144.